Macromolecules

Article

pubs.acs.org/Macromolecules

Rayleigh-Instability-Driven Morphology Transformation by Thermally Annealing Electrospun Polymer Fibers on Substrates

Ping-Wen Fan, Wan-Ling Chen, Ting-Hsien Lee, Yu-Jing Chiu, and Jiun-Tai Chen*

Department of Applied Chemistry, National Chiao Tung University, Hsinchu, Taiwan 30050

Supporting Information

ABSTRACT: Electrospinning has been widely used to prepare polymer fibers with diameters ranging from a few nanometers to micrometers. While most studies focus on controlling the sizes and morphologies of electrospun polymer fibers by changing electrospinning conditions, the effect of post-treatments such as thermal annealing on the properties of electrospun polymer fibers has been less studied. Here, we investigate the effect of thermal annealing on the morphology changes of electrospun polystyrene (PS) fibers on substrates. Different from annealing the fibers in a uniform environment, annealing the fibers on substrates results in a substrate-dependent morphology transformation. When the electrospun PS fibers are annealed on a glass substrate, wetting of the fibers on the glass substrate occurs. When the electrospun PS fibers are annealed on a poly(methyl methacrylate) (PMMA)-coated substrate, a Rayleigh-instability-driven morphology transformation is observed. The polymer fibers transform into hemispherical polymer particles caused by the lower surface tension of PS than that of PMMA and the interfacial tension between PS and PMMA. This transformation process is influenced by the annealing time and temperature. The characteristic time of the transformation process is shorter when the sample is annealed at a higher temperature because of the lower polymer viscosity. The size of the polymer particles fits well with the theoretical prediction, which is dependent on the initial fiber diameter and is independent of the annealing temperature.

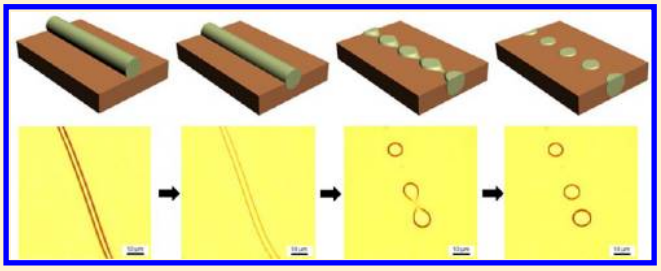

INTRODUCTION

In recent years, the electrospinning process has aroused great interest as a convenient and attractive technique for fabricating polymer fibers with diameters ranging from micrometer to nanometer scales.[1,2] Electrospun polymer fibers have been exploited for applications such as sensors,[3] filtration,[4] wound dressings,[5] drug delivery,[6] or tissue engineering.[7] For these applications, it is desirable to control the sizes and morphologies of the electrospun polymer fibers. Most studies to control the sizes and morphologies of the electrospun fibers focus on changing the experimental parameters during the electrospinning process. These parameters include the type of polymer, the polymer molecular weight, the type of solvent, the solution concentration, the applied voltage, the working distance, or the flow rate. The effect of post-treatments on the size and morphology changes of the electrospun fibers, however, has been poorly studied.

Different post-treatment techniques have been applied to polymer bulks or polymer thin films. Two of the commonly used post-treatment techniques are thermal annealing and solvent annealing.[8,9] During the annealing process, polymer chains are mobile and are capable of achieving their equilibrium conformations.[10,11] Some works have been performed to study the morphologies and properties of electrospun polymer fibers by post-treatments such as thermal annealing. For example, Lim et al. reported that the morphology of electrospun poly(L-lactic acid) (PLLA) nanofibers was changed from a purely fibrillar structure to a mixture of nanogranular and fibrillar structure with enhanced interfibrillar bonding after thermal annealing.[12] The Young's modulus of the nanofibers was increased mainly because of the increase of the crystallinity. Liu et al. also studied that the metastable γ-crystals of electrospun nylon-6 fibers melted and recrystallized into thermodynamically stable α-form crystals after thermal annealing.[13] Despites these works, the annealing effect on the size and morphology changes of electrospun polymer fibers still require further investigation. Recently, we reported the transforming process of electrospun poly(methyl methacrylate) (PMMA) fibers under thermal annealing in ethylene glycol.[14] The surfaces of the PMMA fibers undulate, and the fibers transform into polymer microspheres driven by the interfacial tension between polymer and ethylene glycol. The kinetics of the transformation process was found to be dependent on the annealing conditions such as the annealing time or the annealing temperature.[14] Ethylene glycol does not dissolve PMMA and provides an environment for annealing the PMMA fibers uniformly.[15] Therefore, substrates are not involved in the annealing process, and the main interface to be considered is the interface between polymer and ethylene glycol.

Received: May 14, 2012
Revised: June 23, 2012
Published: July 12, 2012

Here, we investigate the effect of thermal annealing on the size and morphology changes of electrospun polystyrene (PS) fibers on substrates. Different from annealing the fibers in a uniform environment, the type of substrates plays an important role in the annealing process. When the electrospun PS fibers are annealed on a glass substrate, wetting of the PS fibers occurs. When the electrospun PS fibers are annealed on a PMMA-coated substrate, PS fibers transform into hemispherical polymer particles, driven by the Rayleigh instability and the lower surface energy of PS than that of PMMA.

The Rayleigh instability is generally considered when a liquid cylinder is evolved into a row of droplets. This phenomenon is commonly experienced in daily life, as a stream of water flowing from a faucet. The water stream breaks into individual droplets during falling. Joseph Plateau first studied this type of instability in liquid cylinders.[16] He reported that if the wavelength (λ) of a undulation is larger than the perimeter ($2\pi R_0$) of a liquid cylinder, the free surface of the cylinder undulates and disintegrates into a chain of drops.[17] Lord Rayleigh further showed that the wavelength of the undulation is determined by the fastest distortion mode.[18] Rayleigh's theory was applied to solid cylinders by Nichols and Mullins, who used similar calculations.[19] They considered the mass transport of solid cylinders and obtained first-order perturbation solutions for surface diffusion and volume diffusion. For an infinitely long cylinder of radius of R_0, an infinitesimal longitudinal sinusoidal perturbation is introduced. The perturbed surface can be expressed as the equation

$$r = R_0 + \delta \sin(2\pi/\lambda)z \quad (1)$$

where λ is the wavelength, δ is the amplitude of the perturbation, and z is the coordinate along the cylinder axis.[20] For surface diffusion, which dominates in most cases, the amplitude of a perturbation with a wavelength greater than $\lambda_0 = 2\pi R_0$ is unstable and is expected to increase spontaneously with time. But the perturbation with a wavelength $\lambda_m = 8.89R_0$ yields the maximum growth rate.[19] The cylinder finally breaks up into spheres with an average diameter $d = 3.78R_0$. The Rayleigh-instability-driven transformation is observed not only for simple liquids but also for viscoelastic materials such as polymers.[21,22]

When electrospun PS fibers are annealed on PMMA-coated substrates and transform into polymer particles, the condition is different from the original assumption of the Rayleigh instability because more interfaces are considered. The interfaces need to be considered during the transforming process involve the interface between PS and air, the interface between PMMA and air, and the interface between PS and PMMA. By annealing, PS fibers first sink into the PMMA film to reduce the surface area between air and polymers. The fibers then undulate and transform into hemispherical particles, caused by the lower surface tension of PS and the reduction of the interfacial energy between PS and PMMA. The sizes of the particles fit well with the theoretical calculation. The characteristic times for the morphology to change are influenced by the annealing temperature. Shorter times are observed at higher annealing temperatures due to the lower polymer viscosity.

EXPERIMENTAL SECTION

Materials. Polystyrene (PS) and poly(methyl methacrylate) (PMMA) were purchased from Sigma-Aldrich with weight-average molecular weights (M_w) of 192 and 75 kg/mol, respectively. Dimethylformamide (DMF) was obtained from Tedia. The glass substrates were purchased from the FEA Company.

PS Fibers by Electrospinning. In a typical electrospinning experiment to fabricate electrospun PS fibers, a PS solution (30 wt % in DMF) was added into a syringe which was connected to a capillary nozzle (inner diameter: 0.41 mm).[23] The capillary nozzle was connected to a high-voltage power supply (SIMCO), with a voltage range of 10−30 kV. The flow rate of the PS solution was controlled by a syringe pump (KD Scientific) at a constant rate of 1 mL/h. The working distance between the grounded collector and the nozzle was set at 15 cm. Under these conditions, the average diameter of the electrospun polystyrene fibers is ∼6.67 μm with a standard deviation of 0.78 μm. The electrospinning process was carried out at room temperature in a vertical spinning configuration.[23]

Thermal Annealing Process of Electrospun PS Fibers on Substrates. After the electrospinning process, the PS fibers were collected and placed on either glass or PMMA-coated substrates. To prepare the PMMA-coated substrates, a blade coating method was used using a PMMA solution (20 wt % in THF). A PMMA film with a thickness of ∼24 μm was obtained after the evaporation of the solvent. The PS fibers placed on the substrates were thermally annealed by a heating stage equipped with an optical microscope for different temperatures and times. Experimental parameters such as the heating rate, the initial temperature, the final temperature, and the annealing time were controlled. To selectively remove the PMMA layer, the sample was dipped into acetic acid and was washed with water before filtration.

Structure Analysis and Characterization. The glass transition temperatures (T_g) of PS and PMMA were determined by differential scanning calorimetry (DSC) (Seiko Instruments, EXSTAR 6000). A scanning electron microscope (SEM) (JEOL, JSM-7401F) with an accelerating voltage of 10 kV was used to investigate the as-spun polymer fibers. The fibers were dried in a vacuum oven at 30 °C and were coated with 4 nm platinum before the SEM measurement. The structure transformation of the electrospun fibers by thermal annealing were characterized by an optical microscope (OM) (Zeiss) under projector lens (40×) and condenser lens (10×). The annealing temperatures and times were controlled by a temperature controller (Mettler). The in-situ images and movies from OM were collected by an image software (Upmost). A Veeco diInnova atomic force microscope (AFM) under a tapping mode was used to study the surface morphology of the annealed samples.

RESULTS AND DISCUSSION

Figure 1 shows the experimental scheme in this study which contains two major routes. Both routes require the preparation of the polymer fibers by electrospinning. The sizes of the as-spun fibers can be controlled by changing the electrospinning conditions, such as the polymer concentration, the flow rate, or the applied voltage. After the polymer fibers are collected, they are placed on either glass substrates or PMMA-coated

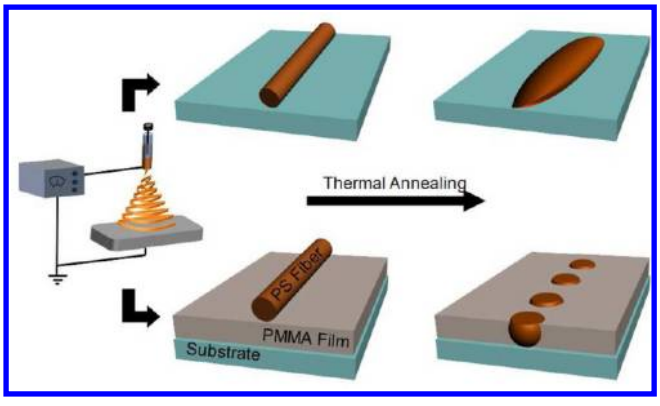

Figure 1. Schematic illustration of the electrospinning and annealing processes of electrospun PS fibers.

dx.doi.org/10.1021/ma300964y | Macromolecules 2012, 45, 5816−5822

substrates, followed by annealing processes under different conditions. When polymers are annealed at temperatures higher than their glass transition temperatures (T_g), they become mobile and are able to achieve their equilibrium morphology. The morphology change of the polymer fibers after thermal annealing depends on the types of the substrates. When PS fibers are annealed on a glass substrate, wetting occurs. When the PS fibers are annealed on a PMMA-coated glass substrate, the PS fibers transform into hemispherical polymer particles driven by the Rayleigh instability and the lower surface tension of PS.

Electrospinning is a convenient technique to prepare polymer fibers. Most polymers can be made as fibers by electrospinning once suitable solvents are used. The sizes and morphologies of the as-spun polymer fibers can be controlled by experimental parameters in the electrospinning process. These experimental parameters include the type of solvent, the type of polymer, the polymer molecular weight, the polymer concentration, the applied voltage, the flow rate, or the working distance.[1] The polymer solution is ejected from a capillary nozzle while a high voltage is applied between the capillary nozzle and the ground collector. A droplet held by the surface tension at the end of the nozzle is subjected to the electric field. When the electric field increases, the droplet is destabilized and coverts into a conical shape referred to as the Taylor cone, with a half-angle of 49.3°.[24] When the electric field is higher than a critical value, the electrostatic force is strong enough to overcome the surface tension force, resulting in the formation of a charged jet of the polymer solution at the bottom of the droplet. The jet becomes thinner because of the bending instability of the electrified jet. After the evaporation of the solvent, the polymer jet solidifies and forms fibers on the collector.

Dimethylformamide (DMF), a commonly used solvent for electrospinning polymer fibers, is used in this work for electrospinning PS fibers.[25] Figure 2 shows the SEM images of electrospun PS fibers prepared under different electrospinning conditions. One simple way to control the size and morphology of the electrospun fibers is by changing the polymer concentration, as the solution viscosity increases with the polymer concentration. At a lower polymer concentration, the viscosity of the polymer solution might be not enough to form a stable jet, resulting in the formation of droplets. At a higher polymer concentration, a stable jet is able to be formed due to polymer entanglements. It has been studied that the fiber diameter increases with the polymer concentration based on a power law relationship.[26] Figures 2a–c show the SEM images of PS fibers prepared from different concentrations while keeping all other experimental parameters constant. Polystyrene (PS) (M_w: 192K) is dissolved in DMF at different concentrations (Figure 2a: 20 wt %; Figure 2b: 25 wt %; Figure 2c: 30 wt %) with the flow rate of 1 mL/h and working distance of 20 cm under the voltage of 10 kV. At lower polymer concentrations, beads-on-string structures are observed because of the contraction of the jet and the entanglement of polymer chains, as shown in Figure 2a.[27] At higher polymer concentrations, polymer fibers without beaded defects can be formed. The diameters of the electrospun PS fibers are found to increase from ~2 μm for 20 wt % to ~5 μm for 30 wt %. With higher polymer concentrations, the diameters of the electrospun fibers can become even larger, but the high viscosity increases the difficulty to eject the solution from the capillary nozzle. In addition, the polymer concentration is also limited by the solubility of the polymers. Other ways to control the solution viscosity include the polymer molecular weight, the molecular weight distribution, the solvent, and the temperature.[28] Gupta et al. studied that the onset of uniform fiber formation of a narrower molecular weight distribution occurs at a lower concentration. This observation was explained by the narrow distribution of hydrodynamic radii and relaxation times of polymers chains with a narrow molecular weight distribution.[28]

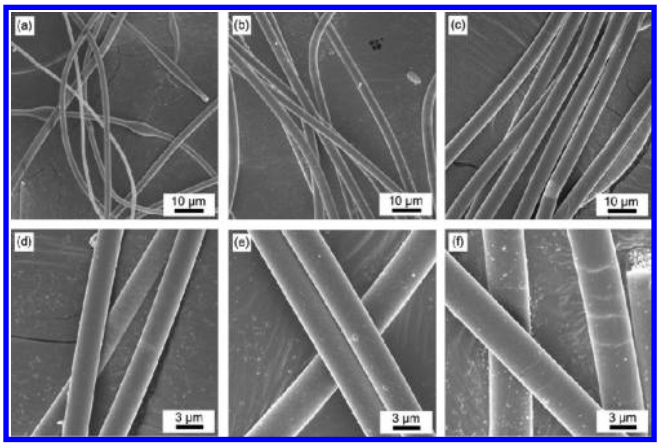

Figure 2. SEM images of electrospun PS (M_w: 192 kg/mol) fibers prepared at different electrospinning conditions. The working voltage and working distance are 10 kV and 20 cm, respectively. (a–c) PS in DMF with flow rate of 1 mL/h at different concentrations: (a) 20, (b) 25, and (c) 30 wt %. (d–f) 25 wt % PS in DMF at different flow rates: (d) 1, (e) 3, and (f) 5 mL/h.

The fiber diameters can also be controlled by changing the flow rate of the polymer solution. More polymer fibers are generated by increasing the flow rate. As the flow rate increases, the diameter of the electrospun fibers also increases. But beaded fibers might be formed at high flow rates. Figures 2d–f show the SEM images of electrospun PS fibers prepared from different flow rates while keeping all other experimental parameters constant. Polystyrene (PS) (M_w: 192K) is dissolved in DMF at the concentration of 25 wt %. Different flow rates (Figure 2d: 1 mL/h; Figure 2e: 3 mL/h; Figure 2f: 5 mL/h) are used, and the working distance is 20 cm under the voltage of 10 kV. The diameters of the electrospun PS fibers are found to increase from ~3 μm for 1 mL/h to ~5 μm for 5 mL/h. The diameters of the electrospun polymer fibers can also be controlled by changing other experimental parameters such as the applied voltage. At higher applied voltages, stronger electric field and electrostatic force are established, resulting in the formation of fibers with smaller diameters.[29] Stronger electric fields can also be achieved by using shorter working distances. But the evaporation of solvent of the solution jet is also affected by the working distance. A shorter working distance may cause insufficient evaporation of the solvent.

When polymer chains are annealed at temperatures above their glass transition temperatures, they are mobile and are capable of achieving a more stable state. In this work, we study the annealing effect on electrospun PS fibers placed on two different substrates. The first substrate is a glass substrate, and the second substrate is a PMMA-coated glass substrate. Figure 3 shows the OM images of electrospun PS fibers thermally annealed on a glass substrate at 240 °C for different periods of time. The polymer fibers are found to wet the glass substrate.

dx.doi.org/10.1021/ma300964y | Macromolecules 2012, 45, 5816–5822

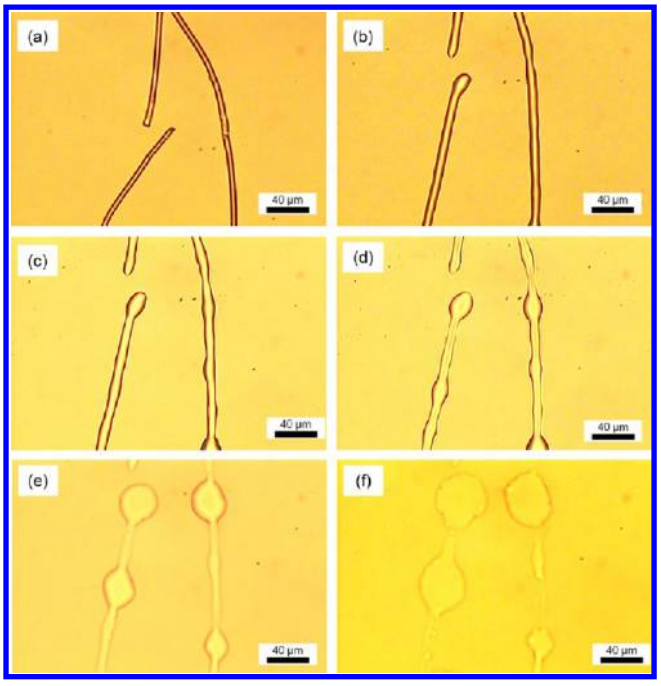

Figure 3. OM images of electrospun PS fibers annealed on a glass substrate at 240 °C for different periods of time: (a) 0, (b) 3, (c) 9, (d) 18, (e) 34, and (f) 45 min. The scale bars for all images are 40 μm.

The wetting behavior of a liquid on a substrate can be estimated by the spreading coefficient S, given by

$$S = \gamma_{SG} - \gamma_{SL} - \gamma \quad (2)$$

where γ_{SG}, γ_{SL}, and γ are the interfacial tensions of solid−gas, solid−liquid, and liquid−gas, respectively. The S value represents the difference of interfacial energies before and after the substrate is covered with a liquid. If S is positive, total wetting occurs, and the substrate is covered with a wetting layer of polymer. If S is negative, the liquid wets the substrate partially with a contact angle θ, defined by the Young's equation: $\theta = \cos^{-1}((\gamma_{SG} - \gamma_{SL})/\gamma)$. The liquid is referred to as "mostly wetting" if θ is smaller than $\pi/2$ and as "mostly nonwetting" if θ is larger than $\pi/2$.[17] The glass substrate has a high surface tension (54.9 dyn/cm) and is wettable by liquids with lower surface tension such as polymer melts. PS has a lower surface tension (40.7 dyn/cm at 20 °C and 32.1 dyn/cm at 140 °C) than that of the glass substrate, and the PS fibers wet the glass substrate after thermal annealing, as shown in Figure 3. We find that the wetting occurs in a shorter time when the fibers are annealed at higher annealing temperatures because of the lower polymer viscosity. It has to be noted that the wetting does not occurs uniformly along the fiber. This is because that the electrospun fibers are not straight, and only parts of the fibers are in direct contact with the substrate.

The thermal annealing process is also performed for PS fibers placed on PMMA-coated glass substrates. Figure 4 shows the OM images of electrospun PS fibers annealed on a PMMA-coated glass substrate at 240 °C for different periods of time. The OM images at higher magnifications are also shown in Figure 5, in which the detail transformation process can be observed. When the polymer fibers are annealed at temperatures from 90 to 250 °C with a heating rate of 5 °C/min, a similar transformation process is also observed (see Figure S1 in the Supporting Information). The glass transition temperatures (T_g) of PS and PMMA are 107 and 105 °C, respectively, determined by the differential scanning calorimetry. The annealing temperature is far above the glass transition temperatures of PS and PMMA. After thermal annealing, the electrospun PS fibers undulate and transform into polymer particles, while the presence of PMMA also affects the transforming process.

This transforming process is similar to our previous results by annealing electrospun fibers in ethylene glycol.[14] When electrospun polymer fibers are annealed in ethylene glycol, the driving force for the fibers to transform into spheres is the minimization of the interfacial energy between polymer and ethylene glycol. In this work, however, more interfaces are involved in the transforming process, and the transformation process is mainly driven by both the Rayleigh instability and the lower surface tension of PS (γ = 40.7 dyn/cm) than that of PMMA (γ = 41.1 dyn/cm). In our previous work to study the transformation process from fibers to spheres annealed in ethylene glycol, the intermediate undulated state is difficult to be observed.[14] In this work, however, in-situ transformation processes of the electrospun fibers can be easily studied by using OM. It has to be noted that dewetting of PMMA on the glass substrate does not occur after annealing at 240 °C because of the large thickness of the PMMA film (thickness ~24 μm) as

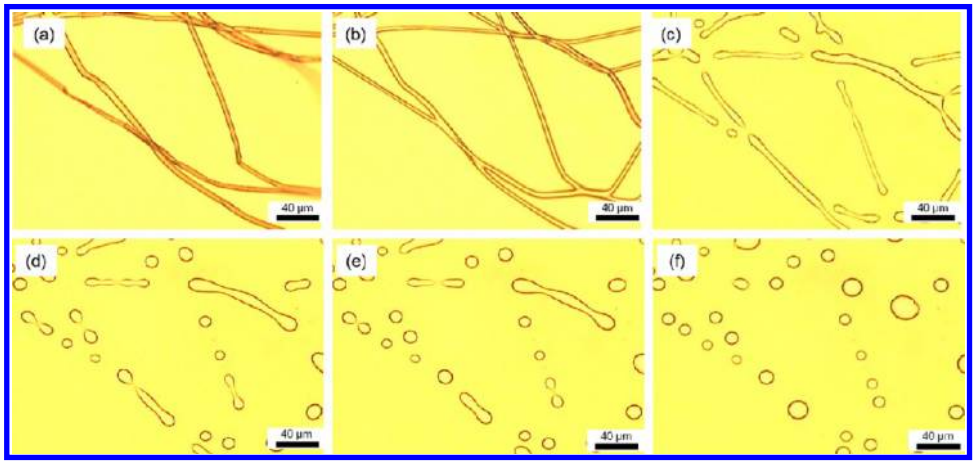

Figure 4. OM images of electrospun PS fibers annealed on a PMMA-coated glass substrate at 240 °C for different periods of time: (a) 0, (b) 34, (c) 146, (d) 178, (e) 188, and (f) 382 s. The scale bars for all images are 40 μm.

dx.doi.org/10.1021/ma300964y | Macromolecules 2012, 45, 5816−5822

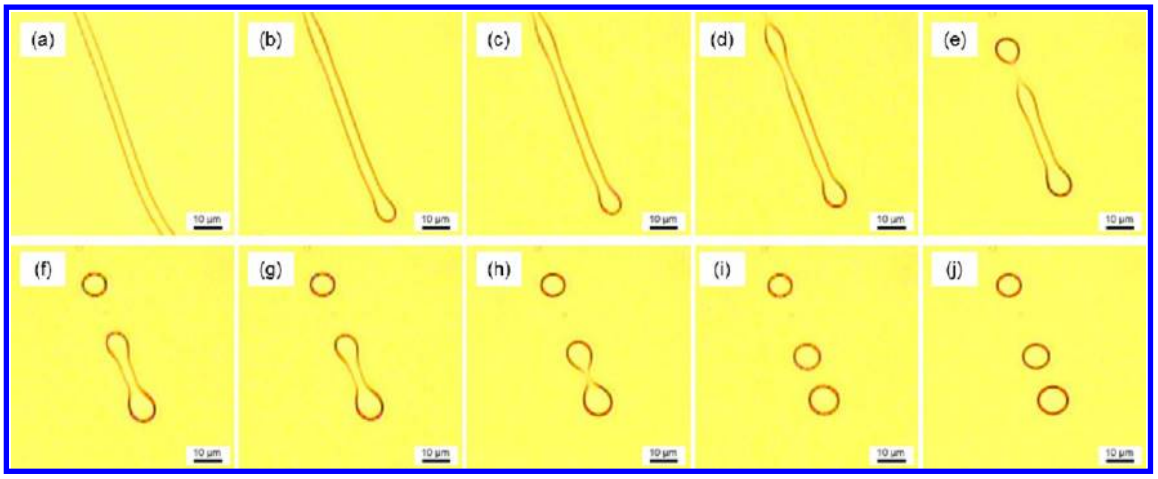

Figure 5. OM images of an electrospun PS fiber annealed on PMMA-coated glass substrate at 240 °C for different periods of time: (a) 124, (b) 140, (c) 146, (d) 154, (e) 166, (f) 176, (g) 180, (h) 188, (i) 196, and (j) 214 s. The scale bars for all images are 10 μm.

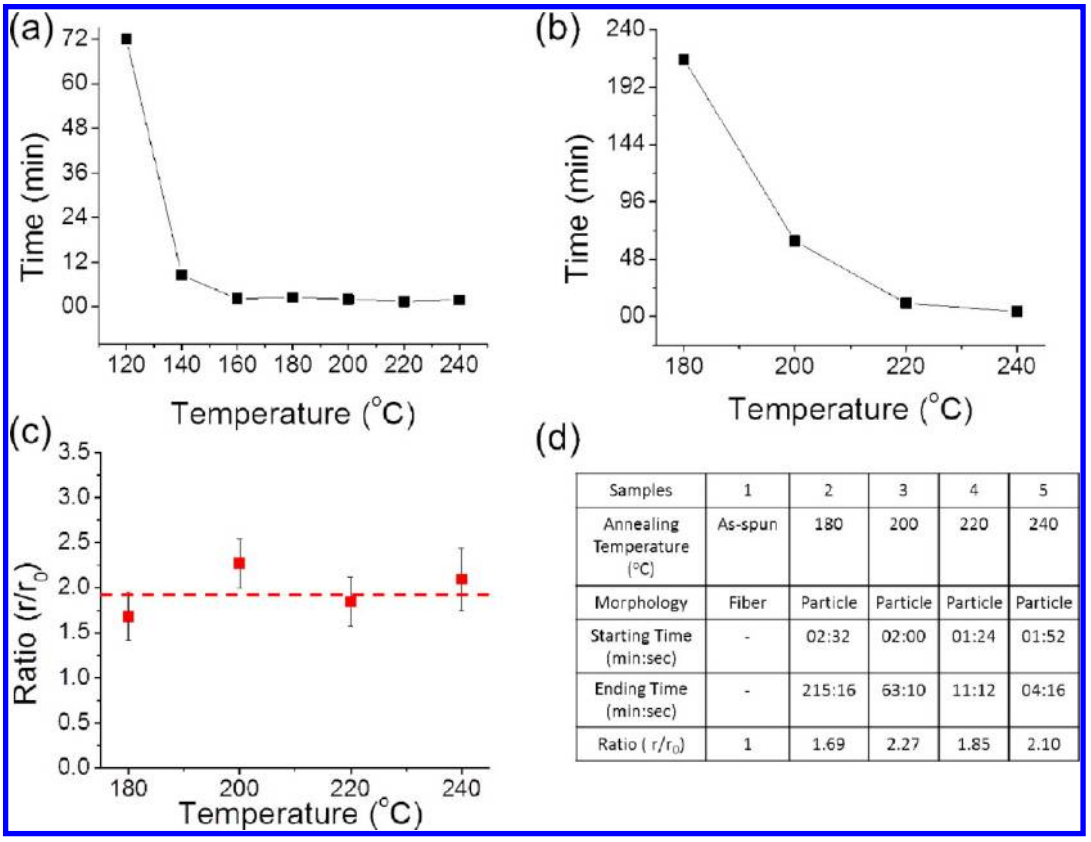

Samples	1	2	3	4	5
Annealing Temperature (°C)	As-spun	180	200	220	240
Morphology	Fiber	Particle	Particle	Particle	Particle
Starting Time (min:sec)	-	02:32	02:00	01:24	01:52
Ending Time (min:sec)	-	215:16	63:10	11:12	04:16
Ratio (r/r_0)	1	1.69	2.27	1.85	2.10

Figure 6. (a) A plot of the annealing temperature versus the starting time of the transformation process. (b) A plot of the annealing temperature versus the ending time of the transformation process. (c) A plot of the annealing temperature versus the ratio of the radius of polymer particles to the initial radius of polymer fibers. The red dashed-line indicates the calculated value of the ratio at 1.89. The error bars represent the standard deviation. (d) A summary table of the polymer samples annealed at different temperatures.

well as the strong interaction between PMMA and the glass substrate.

The characteristic times for the morphology to change under different annealing conditions are also studied. Figure 6a shows the plot of the annealing temperature versus the time that the undulation of the fiber starts. The characteristic time is longer at a lower annealing temperature. In this study, the annealing temperatures we use are from 120 to 240 °C. With higher annealing temperatures, higher mobilities of polymer chains can be achieved, resulting in faster change of the polymer morphology. Figure 6b shows the plot of the annealing temperature versus the ending time of the transformation process. Longer ending times are also observed at a lower annealing temperature. When the Rayleigh-instability-driven transformation is applied to viscoelastic materials such as polymers, the viscosity of the materials resists the undulation and breakup of the cylinder. The characteristic time of the cylinder breakup is determined by the fast growing mode and was defined as

dx.doi.org/10.1021/ma300964y | *Macromolecules* 2012, 45, 5816−5822

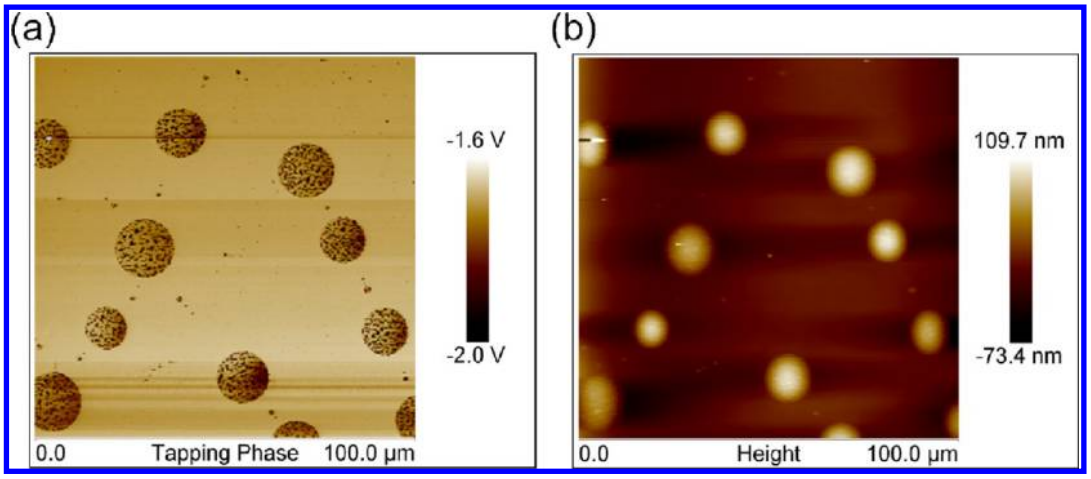

Figure 7. AFM images of electrospun PS fibers annealed on a PMMA-coated glass substrate at 240 °C. (a) The phase image. (b) The height image. The scanned sizes are 100 μm × 100 μm.

$$\tau_m = \eta R_0/\sigma \quad (3)$$

where η is the viscosity, R_0 is the initial radius, τ_m is the characteristic time, and σ is the surface tension of the interface.[30] Therefore, the characteristic time is proportional to the viscosity of the material and should decrease with increasing the annealing temperature, as we find here.

To do a more quantitative study on the transformation process of electrospun fibers, the sizes of the as-spun PS fibers are compared to the sizes of the PS particles. The average diameter of the as-spun PS fibers is ~6.67 μm with the standard deviation of 0.78 μm. According to the theoretical calculations by Nichols and Mullins, perturbations with wavelengths λ_m = $8.89r_0$ have the maximum growth rate, where r_0 is the radius of the cylinder.[19] The amplitude of the perturbation on the cylinder surface increases, and the cylinder disintegrates into particles with an average distance λ_m and an average radius r = $1.89r_0$. Figure 6c is the plot of the annealing temperature versus the ratio of the radius of the polymer particles to the initial radius of the as-spun polymer fibers. The error bars represent the standard deviations, and the red dashed-line indicates the calculated value of the ratio (r/r_0) at 1.89. Compared with the calculated value, the measured ratio of the radius of the polymer particles to the initial radius of the polymer fibers agree well with the theoretical calculations. The measured ratio is also found to be independent with the annealing temperature, implying that the transformation process involves the same pathways even at different annealing temperatures. The sizes and morphologies of the samples annealed at different temperatures are summarized in Figure 6d. Some deviations in the data may be caused by the following reasons: (1) the as-spun PS fibers are not uniform in size; (2) some fibers may overlap and melt together during annealing; (3) fibers are not straight when they are placed on the substrate before annealing.

To further study the morphology of the transformed PS particles, the samples are also examined by AFM. Figure 7 shows the AFM images of electrospun PS fibers annealed on a PMMA-coated glass substrate at 240 °C. The spherical domains in both the phase image and the height image indicate the PS particles. The height of the particles, however, is only 100−200 nm, considerably less than the diameter of the particles (~5−10 μm). Therefore, we claim that one side of the PS particle which exposes to air is slightly elevated, while the other side of the particle is spherical. In the AFM images, some irregular dots on the PS particles are also observed, which might be due to the inhomogeneous heights of the top sides of the PS particles. To confirm the hemispherical shapes of the PS particles, we examine the PS particles by SEM after selectively removing the PMMA layer by acetic acid, a selective solvent for PMMA. As shown in Figure 8, the hemispherical shape of the particle is confirmed, and the size of the particle is ~9 μm, similar to the ones observed by OM.

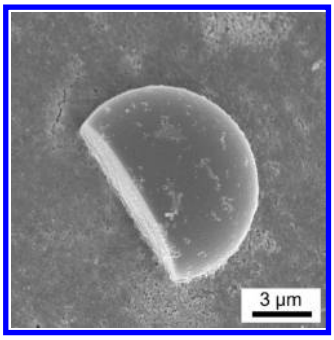

Figure 8. SEM image of a hemispherical PS particle. The particle is obtained by annealing electrospun PS fibers on a PMMA-coated glass at 240 °C, followed by selectively removing PMMA by acetic acid.

The graphical illustrations and corresponding OM images of the transformation process from polymer fibers to polymer particles are shown in Figure 9. The PS fibers first sink into the PMMA films to reduce the surface area between polymers and air. Then the PS fibers undulate and transform into hemispherical particles, caused by the lower surface tension of PS and the reduction of the interfacial energy between PS and PMMA.

■ CONCLUSION

In conclusion, we study the effect of thermal annealing on electrospun PS fibers placed on different substrates. The type of substrates is critical in the annealing process. By using optical microscope, in-situ studies are performed to observe the morphology change during the annealing process. When the PS fibers are annealed on a glass substrate, wetting is observed because of the high surface energy of the glass substrate. When the PS fibers are annealed on a PMMA-coated glass substrate, the fibers transform into hemispherical particles driven by both

dx.doi.org/10.1021/ma300964y | Macromolecules 2012, 45, 5816−5822

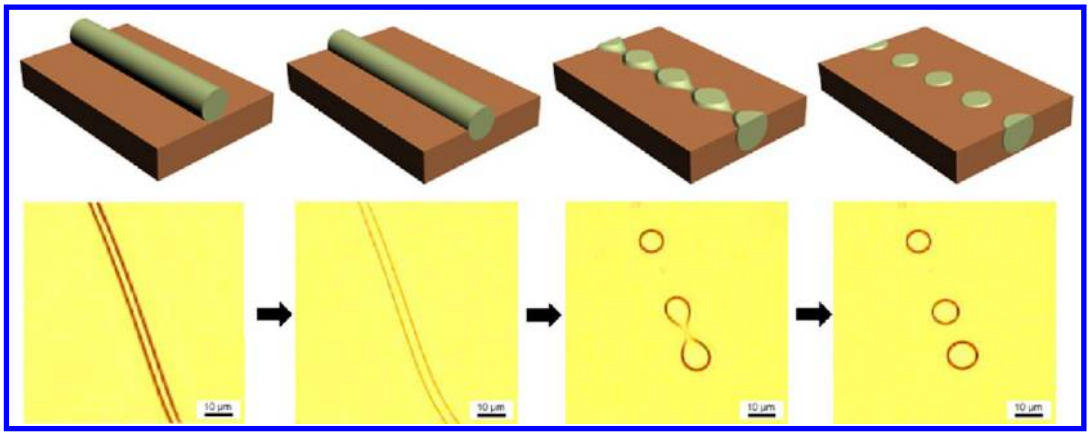

Figure 9. Graphical illustrations and corresponding OM images of the transformation process from polymer fibers to polymer particles.

the Rayleigh instability and the lower surface tension of PS. The morphology transformation is controlled by the annealing conditions such as the annealing temperature and time. At higher annealing temperatures, shorter annealing times are required to transform the fibers into particles. The sizes of the particles fit well with the theoretical calculations and mainly depend on the initial fiber diameter.

For possible future work, we would like to study how the transforming process is affected by other effects such as the type of polymers, the molecular weight, or the molecular weight distribution. In addition, this concept can also be used to prepare hemispherical particles of conjugated polymers or inorganic materials.[31]

■ ASSOCIATED CONTENT

Supporting Information

OM images of annealed PS fibers. This material is available free of charge via the Internet at http://pubs.acs.org.

■ AUTHOR INFORMATION

Corresponding Author

*E-mail: jtchen@mail.nctu.edu.tw; Tel: 886-3-5731631.

Notes

The authors declare no competing financial interest.

■ ACKNOWLEDGMENTS

This work was supported by the National Science Council.

■ REFERENCES

(1) Greiner, A.; Wendorff, J. H. *Angew. Chem., Int. Ed.* **2007**, *46*, 5670−5703.
(2) Huang, Z. M.; Zhang, Y. Z.; Kotaki, M.; Ramakrishna, S. *Compos. Sci. Technol.* **2003**, *63*, 2223−2253.
(3) Rojas, R.; Pinto, N. J. *IEEE Sens. J.* **2008**, *8*, 951−953.
(4) Qin, X. H.; Wang, S. Y. *J. Appl. Polym. Sci.* **2006**, *102*, 1285−1290.
(5) Ignatova, M.; Manolova, N.; Rashkov, I. *Eur. Polym. J.* **2007**, *43*, 1609−1623.
(6) Ashammakhi, N.; Wimpenny, I.; Nikkola, L.; Yang, Y. *J. Biomed. Nanotechnol.* **2009**, *5*, 1−19.
(7) Pham, Q. P.; Sharma, U.; Mikos, A. G. *Tissue Eng.* **2006**, *12*, 1197−1211.
(8) Hodge, I. M. *Macromolecules* **1987**, *20*, 2897−2908.
(9) Kim, Y.; Choulis, S. A.; Nelson, J.; Bradley, D. D. C.; Cook, S.; Durrant, J. R. *Appl. Phys. Lett.* **2005**, *86*, 3.
(10) Zhang, M. F.; Dobriyal, P.; Chen, J. T.; Russell, T. P.; Olmo, J.; Merry, A. *Nano Lett.* **2006**, *6*, 1075−1079.
(11) Chen, J. T.; Chen, D.; Russell, T. P. *Langmuir* **2009**, *25*, 4331−4335.
(12) Tan, E. P. S.; Lim, C. T. *Nanotechnology* **2006**, *17*, 2649−2654.
(13) Liu, Y.; Cui, L.; Guan, F. X.; Gao, Y.; Hedin, N. E.; Zhu, L.; Fong, H. *Macromolecules* **2007**, *40*, 6283−6290.
(14) Fan, P. W.; Chen, W. L.; Lee, T. H.; Chen, J. T. *Macromol. Rapid Commun.* **2012**, *33*, 343−349.
(15) Chen, D.; Park, S.; Chen, J. T.; Redston, E.; Russell, T. P. *ACS Nano* **2009**, *3*, 2827−2833.
(16) Plateau, J. *Transl. Annu. Rep. Simthsonian Inst.* **1873**, 1863−1866.
(17) de Gennes, P. G.; Brochard-Wyart, F.; Quere, D. *Capillarity and Wetting Phenomena*; Springer: New York, 2004.
(18) Rayleigh, L. *Proc. London Math. Soc.* **1878**, *10*, 4−13.
(19) Nichols, F. A.; Mullins, W. W. *Trans. Met. Soc. AIME* **1965**, *233*, 1840−1848.
(20) Karim, S.; Toimil-Molares, M. E.; Balogh, A. G.; Ensinger, W.; Cornelius, T. W.; Khan, E. U.; Neumann, R. *Nanotechnology* **2006**, *17*, 5954−5959.
(21) Chen, J. T.; Zhang, M. F.; Russell, T. P. *Nano Lett.* **2007**, *7*, 183−187.
(22) Chen, D.; Chen, J. T.; Glogowski, E.; Emrick, T.; Russell, T. P. *Macromol. Rapid Commun.* **2009**, *30*, 377−383.
(23) Chen, J. T.; Chen, W. L.; Fan, P. W. *ACS Macro Lett.* **2012**, *1*, 41−46.
(24) Taylor, G. *Proc. R. Soc. London, A* **1969**, *313*, 453−475.
(25) Wannatong, L.; Sirivat, A.; Supaphol, P. *Polym. Int.* **2004**, *53*, 1851−1859.
(26) Deitzel, J. M.; Kleinmeyer, J.; Harris, D.; Tan, N. C. B. *Polymer* **2001**, *42*, 261−272.
(27) Fong, H.; Chun, I.; Reneker, D. H. *Polymer* **1999**, *40*, 4585−4592.
(28) Gupta, P.; Elkins, C.; Long, T. E.; Wilkes, G. L. *Polymer* **2005**, *46*, 4799−4810.
(29) Wang, C.; Hsu, C. H.; Lin, J. H. *Macromolecules* **2006**, *39*, 7662−7672.
(30) Edmond, K. V.; Schofield, A. B.; Marquez, M.; Rothstein, J. P.; Dinsmore, A. D. *Langmuir* **2006**, *22*, 9052−9056.
(31) Shen, X. Q.; He, F.; Wu, J. H.; Xu, G. Q.; Yao, S. Q.; Xu, Q. H. *Langmuir* **2011**, *27*, 1739−1744.